International Journal of Pharmaceutics 424 (2012) 89–97

Contents lists available at SciVerse ScienceDirect

International Journal of Pharmaceutics

journal homepage: www.elsevier.com/locate/ijpharm

Pharmaceutical Nanotechnology

The effect of a P123 template in mesopores of mesocellular foam on the controlled-release of venlafaxine

Jing Tang, Zijun Bian, Jun Hu*, Shouhong Xu, Honglai Liu

Key Laboratory for Advanced Materials, Department of Chemistry, East China University of Science and Technology, Shanghai 200237, PR China

ARTICLE INFO

Article history:
Received 26 August 2011
Received in revised form
22 November 2011
Accepted 25 December 2011
Available online 31 December 2011

Keywords:
Mesocellular foam
P123
Controlled-release
Venlafaxine

ABSTRACT

A series of mesocellular foams (MCFs)-based mesoporous silica nanospheres (DH-MCF-P123-*n*, (*n* = 12, 2, 0.5)) were synthesized as controlled-release deliveries for a typical antidepressant drug, venlafaxine. The foams were 3-(2,3-dihydroxypropoxyl)propyl-grafted and the P123 template partially preserved. We studied the release profiles of venlafaxine-loaded DH-MCF-P123-*n* in simulated gastric fluid (SGF) and simulated intestinal fluid (SIF), respectively, as well as their corresponding venlafaxine loading capacities. Appropriate amounts of P123 template preserved in mesopores showed an efficient synergetic effect on increasing venlafaxine loading capacity and controlled-release property. Up to 90.87% (mass fraction) of venlafaxine could be loaded into DH-MCF-P123-2. For this carrier, 36% of venlafaxine was released after 1 h of incubation in SGF and 53% of venlafaxine was released after 12 h in SIF. The mechanisms of the loading and releasing processes were tentatively described based on the release behaviors.

1. Introduction

Over the past few decades, there has been considerable interest in developing drug delivery nanotechnology for small molecules, proteins and DNA (Kim et al., 2009; Sahoo and Labhasetwar, 2003). Nanotechnology-based delivery systems, including polymeric biodegradable nanoparticles (Panyam and Labhasetwar, 2003; Panyam et al., 2002), ceramic nanoparticles (Jain et al., 1998; Roy et al., 2003), polymeric micelles (Hrubý et al., 2005; Lee et al., 2003, 2005), dendrimers (Gillies and Fréchet, 2005; Liu and Fréchet, 1999) and liposomes (Lasic et al., 1999; Park, 2002), have been introduced and designed to respond to specific stimuli, such as electric field (Murdan, 2003), magnetic field (Liu et al., 2008), pH (Gyenes et al., 2008; Yang et al., 2010; Zhu et al., 2005) and temperature (Zhang et al., 2009) to improve the drug efficacy, reduce the drug toxicity and meet the requirement of site-selective and targeted delivery (Sahoo and Labhasetwar, 2003). Polymeric micelles that possess the properties of a fairly narrow size distribution in the nanometer range and the unique core–shell architecture in aqueous solution are able to avoid renal exclusion, clearance by reticuloendothelial system (RES), and provide good endothelial cell permeability (Kataoka et al., 2001; Rosler et al., 2001). They are extensively used as the delivery for water-insoluble drugs, such as anti-tumor drugs (Gou et al., 2011; Matsumura et al., 2004; Nakanishi et al., 2001; Nasongkla et al., 2006; Torchilin et al., 2003; Yokoyama et al., 1998).

Mesoporous silica materials are a kind of ceramic nanoparticles with good biocompatibility, no toxicity, stability and adjustable pore size and structure. They have attracted considerable attention as supports for adsorption and immobilization of biologically relevant molecules (Horcajada et al., 2004; Mal et al., 2003; Pasqua et al., 2007; Slowing et al., 2008; Vivero-Escoto et al., 2010; Xu et al., 2008) since the first report of M41S materials as a drug delivery agent (Vallet-Regí et al., 2000) at the beginning of this century. Among various mesoporous materials, having large pore diameter and interconnected pore structure (Lettow et al., 2000; Schmidt-Winkel et al., 1999, 2000), mesocellular foams (MCFs) extend the delivery application for large biomacromolecules, and raise the drug loading capacity (Zhang et al., 2010, 2011). However, larger pores of MCFs also cause a problem of the drug burst release. The structural template of MCFs, Pluronic $EO_{20}PO_{70}EO_{20}$ (P123), is an amphiphilic poly(ethylene oxide)-b-poly(propylene oxide)-b-poly(ethylene oxide) triblock copolymer that can self-associate to form micelles in aqueous solution and has relatively high biocompatibility (Kabanov et al., 2002). Recently, it was reported that a similar Pluronic triblock copolymer F127 showed positive effects on the controlled-release of cisplatin in a rabbit model (Sonoda et al., 2010). A P123/amorphous calcium phosphate (ACP) nanocomposition was reported as a successful carrier for ibuprofen (Cao et al., 2010). These successful cases aroused our interest in identifying the synergistic effect of the P123 template in

* Corresponding author at: Department of Chemistry, 130 Meilong Road, Shanghai 200237, PR China. Tel.: +86 21 64252922; fax: +86 21 64252922.
E-mail address: junhu@ecust.edu.cn (J. Hu).

0378-5173/$ – see front matter © 2011 Elsevier B.V. All rights reserved.
doi:10.1016/j.ijpharm.2011.12.048

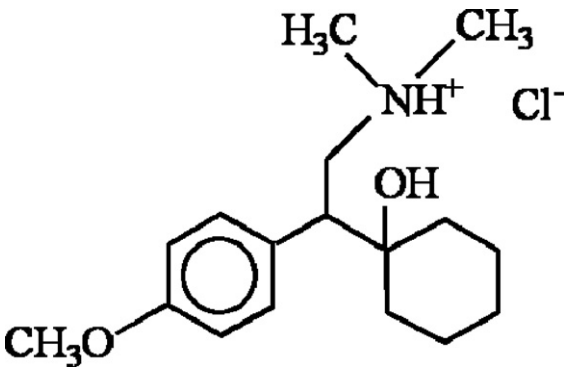

Fig. 1. Molecular structure of Venlafaxine hydrochloride (VenHCl).

mesoporous materials on the controlled-release of drugs. To the best of our knowledge, there are very few reports referring to this special delivery mesoporous material with template partially preserved, although it will be meaningful not only for the controlled-release methodology, but also for the future application and fabrication with the process of removing templates.

A large amount of antidepressants were produced because of the increasing prevalence of major depression worldwide (Gonzalez et al., 2010). Among them, as a bicyclic phenylethylamine derivative (Keltjens et al., 2003; Wellington and Perry, 2001) (Fig. 1), venlafaxine is a typical selective serotonin reuptake inhibitor (SSRI). Although a commercial extended release capsule (EFFEXOR XR®), one of the most commonly prescribed antidepressants on the US retail market in 2007 (Drug Topics, 2008), is already available, it still has some side effects, such as nausea, insomnia, weakness, drowsiness and constipation. Therefore, improving the controlled-release performance of venlafaxine is likely to be a good direction to increase patients' tolerance. In our previous work, poly(lactic acid) was introduced to coat the mesoporous silica nanoparticles (MSN) to improve the controlled-release of venlafaxine (Tang et al., 2011). However, the effect of the P123 template was not investigated.

Herein, MCFs with various amounts of P123 template preserved were synthesized and used as the drug delivery for venlafaxine. The loading capacity and in vitro release in simulated gastric fluid (SGF) and simulated intestinal fluid (SIF) were investigated. The mechanism for the synergistic effect of P123 template on the loading and release processes was also described.

2. Materials and methods

2.1. Materials

Venlafaxine hydrochloride and Pluronic P123 were purchased from Sigma–Aldrich Company. Monobasic potassium phosphate, NaOH, tetraethyl orthosilicate (TEOS) and toluene were purchased from Shanghai Lingfeng Chemical Reagent Co., Ltd. Ethanol (anhydrous), hydrochloric acid and 1,3,5-trimethylbenzene (TMB) were purchased from Sinopharm Chemical Reagent Co., Ltd. (3-Glycidoxypropyl)methyldiethoxysilane was provided by Shanghai Guipu Chemical Reagent Co., Ltd. All reagents were in analytical pure grade and used without further purification except for toluene, which was dehydrated before using.

2.2. Synthesis of MCFs

MCF was synthesized by modifying the conventional MCF synthesis method (Han et al., 2007), in which, Pluronic P123 (8.0 g) was dissolved in a hydrochloric acid solution (150 mL, 1.6 mol L^{-1}) at 40 °C by vigorous stirring. Then TMB (5.0 g) was added. After continuous stirring for 2 h, TEOS (18.4 mL) was added dropwise using a syringe with extra stirring for 5 min. The slurry was transferred into an autoclave and aged at 40 °C for 20 h under a static condition. Then the temperature was increased to 100 °C, and it was aged again for 24 h. The resulting precipitate was filtered, washed with water and ethanol, and dried. The product was denoted as MCF-as.

The above dry MCF-as (1.5 g) was refluxed in a hydrochloric acid ethanol solution (160 mL ethanol mixed with 1.3 mL concentrated HCl) for 12 h to remove the P123 template. Then it was filtered, washed with water and ethanol, and dried. The resulting material was denoted as MCF-P123-12.

2.3. Synthesis of 3-(2,3-dihydroxypropoxyl)propyl-grafted MCFs

The 3-(2,3-dihydroxypropoxyl)propyl-grafted spherical MCF materials were synthesized by the following process: The MCF-as powder (1.0 g), containing P123 template, was dispersed in dry toluene (80 mL), then, (3-glycidoxypropyl)methyldiethoxysilane (1.5 mmol) was injected. The mixture was refluxed overnight under a nitrogen atmosphere. The resulting 3-glycidoxypropyl-grafted MCF-as powder was filtered, washed with toluene and ethanol, and dried. The dry 3-glycidoxypropyl-grafted MCF-as powder (1.5 g) was refluxed in a HCl ethanol solution (160 mL ethanol mixed with 1.3 mL concentrated HCl) for n (n = 12, 2, 0.5) hours to remove (or partially remove) P123 template. The ring cleavage reaction of 3-(2,3-epoxypropoxy)propyl group took place in this HCl ethanol solution to yield 3-(2,3-dihydroxypropoxyl)propyl-grafted MCF materials. Finally, the resulting products (1.0 g) were treated with 80 mL of a 1:7 (v/v) water/ethanol solution of sodium bicarbonate (0.042 g) for 4 h at room temperature to remove any unreacted and physisorbed (3-glycidoxypropyl)methyldiethoxysilane. Then, they were filtered, washed with water and ethanol, and dried. The resulting materials were denoted as DH-MCF-P123-n (n = 12, 2, 0.5).

2.4. Loading venlafaxine

DH-MCF-P123-n (n = 12, 2, 0.5) powder (250 mg) was added into 10 mL venlafaxine (6.0 mg, 19.12 mmol) aqueous solution. The mixture was then sealed and stirred overnight at room temperature. After that, the precipitates were filtered, washed with a small amount of water and dried under vacuum at room temperature. The filtrates were diluted with H_2O to a final volume of 50 mL. The resulting materials were correspondingly denoted as VEN-DH-MCF-P123-n (n = 12, 2, 0.5).

The amounts of venlafaxine loaded in samples (wt) were calculated by Eq. (1) and the loading capacities of venlafaxine (mass fraction) were calculated by Eq. (2).

$$wt = \frac{m_1 - CV}{m_2 + (m_1 - CV)} 1000 \quad (1)$$

$$P\% = \frac{m_1 - CV}{m_1} \times 100 \quad (2)$$

where m_1 and m_2 are the initial mass of venlafaxine and DH-MCF-P123-n, respectively. C is the concentration of the filtrate diluted in 50 mL volumetric flask, and V is the volume of the diluted filtrate (here 50 mL).

2.5. In vitro release of venlafaxine

2.5.1. Preparation of SGF and SIF

Enzyme free SGF was prepared according to United States Pharmacopeia specification (USP-NF, 2005). 0.1 g sodium chloride was dissolved in 40 mL H_2O, and then, 0.35 mL condensed HCl was added, the pH value of this solution was approximately 1.2. Then, the solution was diluted with H_2O to a final volume of 50 mL.

Enzyme free SIF was prepared according to United States Pharmacopeia specification (USP-NF, 2005). 0.68 g monobasic potassium phosphate was dissolved in 25 mL H_2O, and then, 7.7 mL 0.2 mol L^{-1} NaOH and 50 mL H_2O were added. The pH value of this solution was adjusted to 6.8 with 0.2 mol L^{-1} NaOH. After that, the solution was diluted with H_2O to a final volume of 100 mL.

2.5.2. In vitro drug release

The release profiles of venlafaxine were obtained by soaking VEN-DH-MCF-P123-*n* (*n* = 12, 2, 0.5) (4 mg) in a 10.00 mL SGF or a 10.00 mL SIF, respectively. The in vitro release was performed at 37 °C under a constant stirring rate. After each predetermined time interval, the suspension was centrifuged with a rate of 4000 rpm for 5 min, then a 1.00 mL aliquot of supernatant was collected and another 1.00 mL of fresh SGF or SIF was added immediately to keep the volume constant. The concentration of venlafaxine in each supernatant was analyzed by fluorescence spectrophotometry (FS).

The calculation of the corrected amount of venlafaxine released was based on Eq. (3).

$$n_{N\mathrm{corr}} = C_N V + \upsilon \sum_{i=0}^{N-1} C_i, \quad N = 1, 2, 3, \ldots \tag{3}$$

where $n_{N\mathrm{corr}}$ is the corrected amount (mol) at the *N*th collected times, C_N is the drug concentration analyzed by FS at the *N*th collected times, υ is the volume of the supernatant taken (here 1.00 mL), and *V* is the total volume of the release medium (here 10.00 mL).

2.6. Characterization

Powder X-ray diffraction (XRD) measurements were carried out on a D/Max-2550 VB/PC diffractometer (40 kV, 200 mA), using Cu Kα radiation. Nitrogen adsorption/desorption isotherms were obtained on a Micrometritics ASAP 2020 Surface Area and Porosity Analyzer at 77 K. The surface areas were calculated by the Brunauer–Emmett–Teller (BET) equation and the pore size distribution were calculated by a simplified Broekhoff-de Boer (BdB) method using Frenkel–Halsey–Hill (FHH) theory, namely BdB–FHH method (Lukens et al., 1999) and using a Microsoft Excel VBA macro. Thermogravimetric Analysis (TGA) was carried out using a TGA unit (NETZSCH STA 499 F3). About 5 mg of sample was heated from 20 °C to 700 °C with a heating rate of 5 °C min^{-1} and a continuous N_2 purge of a flow rate of 40 mL min^{-1}. The morphology and the particle size of samples were characterized by using a JEM 6360 scanning electron microscope (SEM) instrument (JEOL) operated at 15 kV. The porous structure of the samples was characterized using a JEM

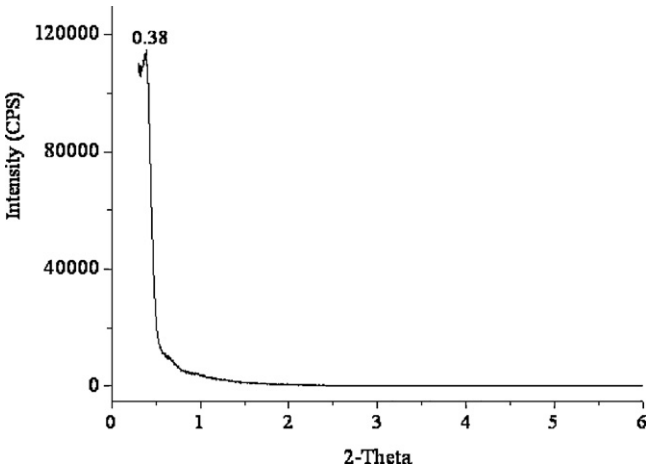

Fig. 2. Powder X-ray diffraction pattern of MCF-P123-12.

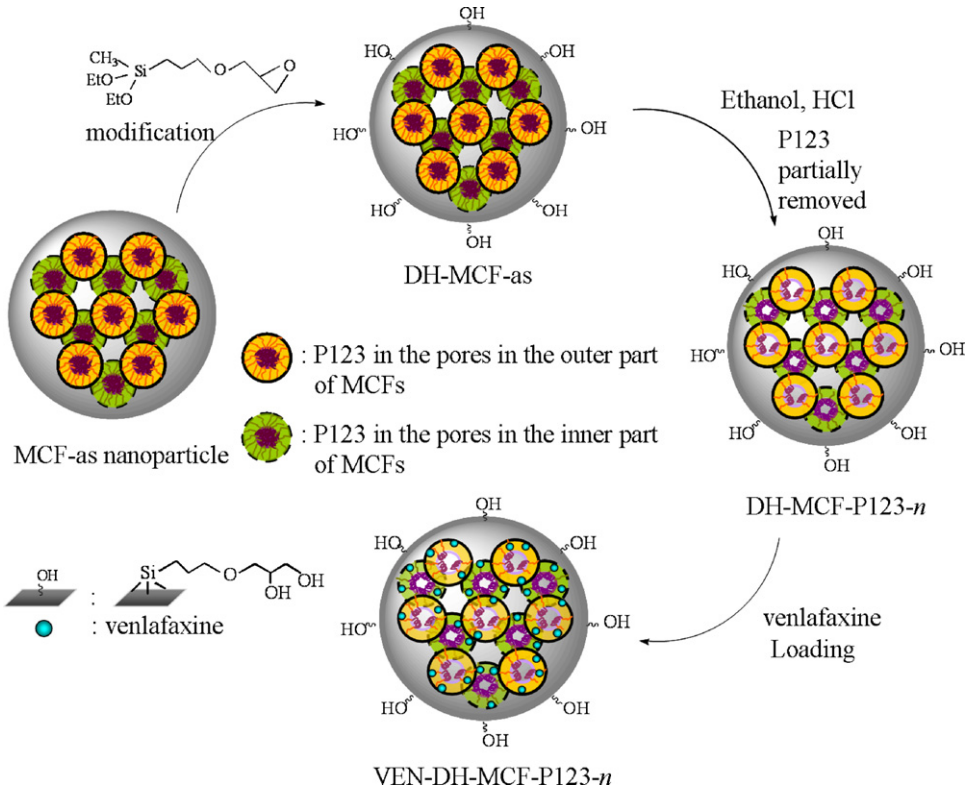

Scheme 1. Schematic representation of the preparation of venlafaxine-loaded MCF nanoparticles with partially removed P123 (VEN-DH-MCF-P123-*n*). (For interpretation of the references to color in text, the reader is referred to the web version of this article.)

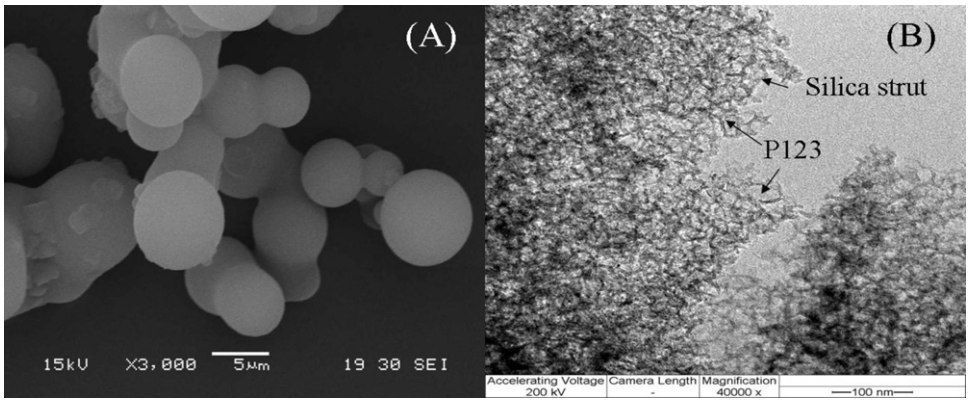

Fig. 3. (A) SEM micrograph and (B) TEM micrograph of MCF-as nanoparticles.

2100 transmission electron microscopy (TEM) instrument (JEOL) operated at 200 kV.

The amount of venlafaxine released was analyzed using a fluorescence spectrophotometer (F4500, HITACHI) at 37 °C. The excitation wavelength was set as 237 nm. Each fluorimetric intensity of released venlafaxine was corrected by analyzing a standard venlafaxine solution (4 μg mL^{-1}). The linear calibration curves were constructed by plotting the fluorescence intensity of the standard venlafaxine solutions (prepared by using SGF and SIF solution, respectively) against the concentration in the range of 0.1–4 μg mL^{-1}. Each data used in this paper was the average value of three repeated measurements.

3. Results and discussion

3.1. Characterization of MCF-P123-12 and DH-MCF-P123-n

Three drug carriers DH-MCF-P123-*n* (*n* = 12, 2, 0.5) with different weight percentages of P123 template preserved were synthesized according to the routes as shown in Scheme 1. The gray area represents the mesostructured silica framework and the colorful micellar structure represents the P123 template in the outer part (light color) and the inner part (dark color) of the MCF particles. The amount of P123 remaining can be adjusted by controlling the extraction time. Finally, the venlafaxine was loaded into the pores.

3.1.1. X-ray diffraction

MCFs have been analyzed using X-ray diffraction. As shown in Fig. 2, there is a characteristic peak at 2θ of 0.38° with high intensity, indicating the existence of the ultra-large mesopores.

3.1.2. TEM and SEM images

The morphology and the structure of the representative MCF-as are illustrated in the SEM image in Fig. 3(A) and the TEM image in Fig. 3(B), respectively. The TEM image gives a clear evidence of the disordered foams of silica struts, which is the characteristic structural feature of the MCF (Schmidt-Winkel et al., 2000). The cell size estimated from TEM is about 30 nm, which is consistent with that determined from nitrogen sorption (D_C of MCF-P123-12 is centered at 32.0 nm) as summarized in Table 1. P123 could be indicated by the lower contrast regions inside the silica struts. The SEM image illustrates that MCF-as is spherical nanoparticles with diameter of 2–8 μm.

3.1.3. Thermogravimetric analysis

MCFs were subjected to thermo-gravimetric and differential thermal simultaneous analyses (TGA/DTA). The weight loss percentage of samples (*C*%) was calculated by Eq. (4).

$$C\% = \frac{m_2 - m_3}{m_1} \times 100 \quad (4)$$

where m_1 is the sample mass after dehydration. m_2 and m_3 correspond to the sample mass before and after the decomposition process, respectively.

Fig. 4 shows the TG curves of series samples. The onsets of the decomposition temperature of P123 and TMB in each sample are all at about 250 °C, however, the weight loss of each sample is different because of its preparation procedure. The values of *C*% of MCFs are listed in Table 1. For MCF-as, it is 24.0%, corresponding to the weight percentage of P123 and TMB in the material. For MCF-P123-12, the weight percentage decreases to 8.6%, corresponding to the weight percentage of remained P123 and TMB in mesopores, which suggests that the most of P123 and TMB can be removed after 12 h extraction process. For the same extraction process, the value of *C*% of DH-MCF-P123-12 increases to 11.7% due to the decomposition of 3-(2,3-dihydroxypropoxyl)propyl layer. For the samples with less extraction time, the values of *C*% of DH-MCF-P123-2 and DH-MCF-P123-0.5 are 13.9 and 17.8, respectively, indicating the amounts of P123 remained in MCFs can be adjusted by controlling the extraction time.

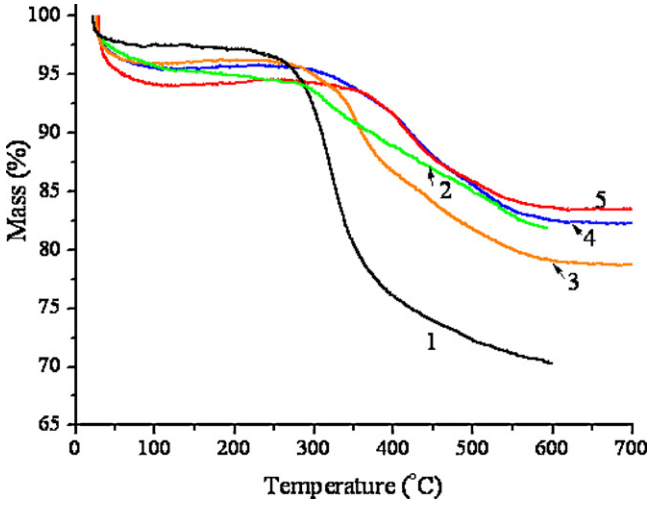

Fig. 4. TG curves of MCFs materials: (1) MCF-as; (2) MCF-P123-12; (3) DH-MCF-P123-0.5; (4) DH-MCF-P123-2; (5) DH-MCF-P123-12.

Table 1
Structural information and venlafaxine loading amount of MCF materials.

Material	C (%)	S_{BET} ($m^2\ g^{-1}$)	V_p ($cm^3\ g^{-1}$)	D_C (nm)	D_W (nm)	wt ($mg\ g^{-1}$)	P (%)
MCF-as	24.0	–	–	–	–	–	
MCF-P123-12	8.6	686.97	2.202	32.0	11.7	–	
DH-MCF-P123-12	11.7	540.38	1.935	29.8	11.7	12.25	80.34
DH-MCF-P123-2	13.9	554.02	1.895	28.9 23.1	11.8	13.60	90.87
DH-MCF-P123-0.5	17.8	442.86	1.628	27.4 24.4	12.4 10.4	3.18	24.53

3.1.4. Nitrogen sorption analysis

Fig. 5 shows nitrogen adsorption/desorption isotherms and their corresponding BdB–FHH cell- and window-size distributions of the materials. All isotherms are of type IV with a H1 type hysteresis loop at high relative pressure, which suggest composition of fairly uniform pore size in spheroidal particles (Gregg and Sing, 1982). For "ink bottle" shape cells, the cell size of a MCF can be determined by the adsorption isotherm of the loop, while the desorption isotherm of the loop leads to determination of "neck" size (Lukens et al., 1999). These "ink bottle" are connected to each other by the "necks". Lukens et al. (1999) created a BdB–FHH method for pore size analysis to avoid the underestimation by using BJH method. Herein, the cell size was determined from the adsorption branch of the isotherms, while the window size was from desorption branch by BdB–FHH method.

The structural parameters of the MCF materials, including BET surface (S_{BET}), pore volume (Vp), cell diameter (D_C) and window diameter (D_W) are summarized in Table 1. The BET surface areas of MCF-P123-12 and DH-MCF-P123-12 are 686.97 $m^2\ g^{-1}$ and 540.38 $m^2\ g^{-1}$, respectively; their D_W distributions are almost the same, both are centered at 11.7 nm. However, the profiles of their D_C distributions are different. As shown in the insets of Fig. 5(a) and (b), there is a sharp peak at 32.0 nm for MCF-P123-12, whereas it is a little smaller (29.8 nm) for DH-MCF-P123-12. Their differences in the surface areas and D_C distributions were attributed to the organosilane modification of 3-(2,3-dihydroxypropoxyl)propyl-grafting. Jaroniec et al. (Antochshuk and Jaroniec, 1999) reported a one-step silylation with both the modification of mesopores and the extraction of template molecules, simultaneously. They suggested that the modification with the organosilane proceed could take place not only on the external surface of the material but also in the mesopores to some extent.

The inserts in Fig. 5(c) and (d) show the pore size distributions of DH-MCF-P123-2 and DH-MCF-P123-0.5. Having less extraction time, P123 micelles in the inner part of the particle were difficult to remove, which resulted in the pore size polydispersion. For the

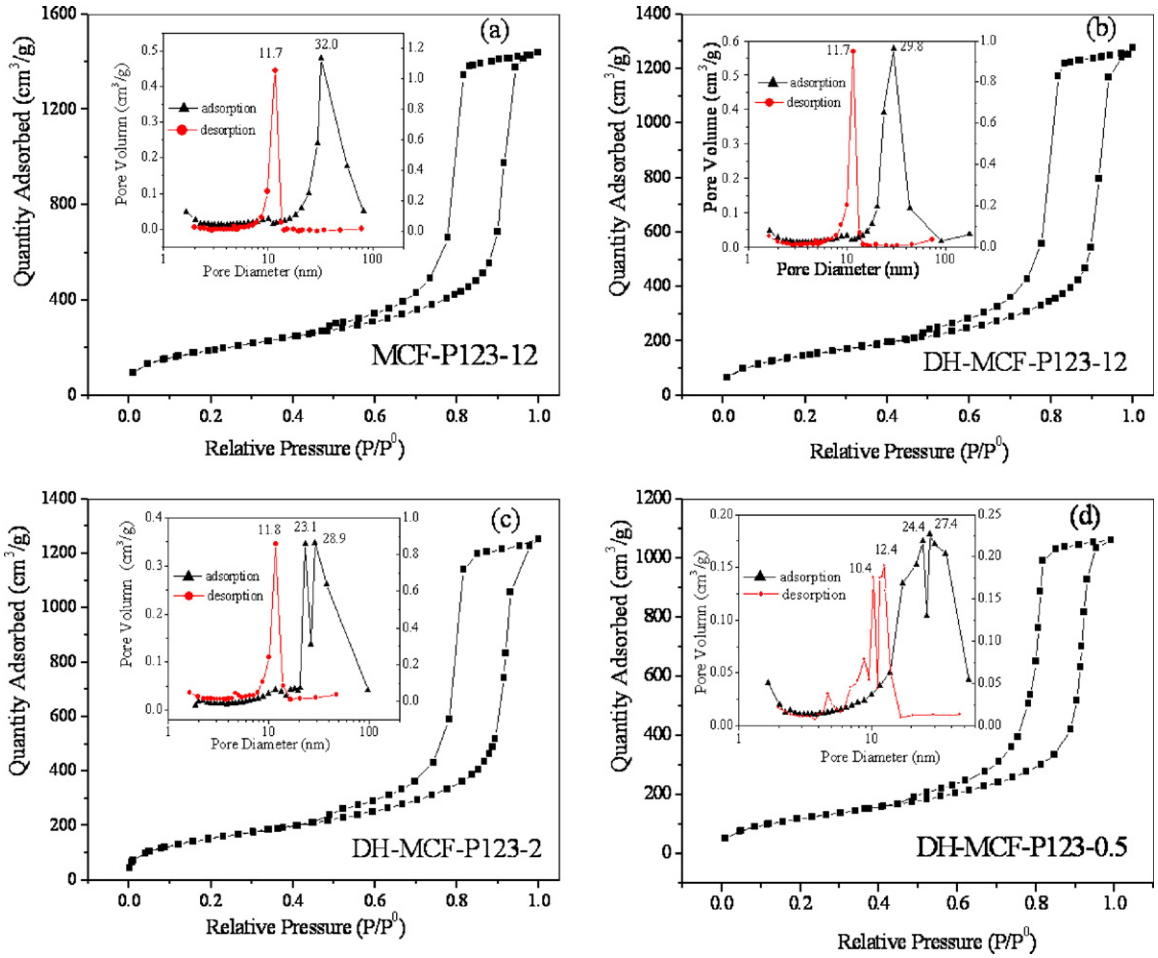

Fig. 5. Nitrogen adsorption/desorption isotherms and corresponding BdB–FHH cell- and window-size distributions of MCFs materials: (a) MCF-P123-12; (b) DH-MCF-P123-12; (c) DH-MCF-P123-2; (d) DH-MCF-P123-0.5.

former one, D_C distribution is centered at two positions of 23.1 and 28.9 nm, smaller than that of DH-MCF-P123-12. It is definitely attributed to the existence of P123 in cells. For the later one, it is more obvious that the distributions of both the cell size and the window size are not unitary. There are two peaks at 24.4 and 27.4 nm for the cell size, and two peaks at 10.4 and 12.4 nm for the window size. The cleavage phenomena are due to the increased amounts of the remaining P123 molecules that are not only in the cells, but also in the windows. Besides, the pore volume decreased with the shortage of the extraction time, correspondingly.

3.1.5. Venlafaxine loading

The amount of venlafaxine loaded (*wt*) and the loading capacity (*P*) of DH-MCF-P123-12, DH-MCF-P123-2 and DH-MCF-P123-0.5 were calculated by Eqs. (1) and (2), respectively. The values were listed in Table 1. 90.87% of venlafaxine can be successfully loaded in DH-MCF-P123-2, with the amount of 13.60 mg venlafaxine per gram DH-MCF-P123-2. A considerable increase or decrease of P123 content remaining in MCFs would both result in the decrease of the loading amount and the loading capacity, which are demonstrated by results from DH-MCF-P123-12 and DH-MCF-P123-0.5. There are two dominant factors in the drug loading process, the free space of carriers and the interaction between drug molecules and carriers. Appropriate amounts of P123 in mesopores could provide sufficient space for drug loading and bring more interaction points between P123 and venlafaxine to increase the loading capacity.

3.2. Release performance of venlafaxine from the MCFs with P123 template in simulated gastrointestinal tract

To study the effect of P123 on controlled-release of venlafaxine, we performed experiments using SGF (pH value is 1.2) and SIF (pH value is 6.8) as the media to mimic the gastric and intestinal environment, respectively.

3.2.1. Fluorescence spectral properties of P123, venlafaxine and their mixture

Venlafaxine shows a strong native fluorescence property (Shahnawaz et al., 2010). In order to eliminate the interference of the fluorescence emission from P123, 3D fluorescence measurements of P123 and venlafaxine were carried out (as shown in Fig. S1). Based on their results, we chose 237 nm as the excitation wavelength for further series of measurements. The fluorescence emission spectra of the P123, venlafaxine and their mixture are shown in Fig. 6. In Fig. 6, curve 1 is the emission spectrum of 1 mg L^{-1} P123 aqueous solution (below the critical micelles concentration (CMC) of P123 (Wanka et al., 1994)), no peak is observed at the range of 280–400 nm. However, when the concentration is increased to 10 mg L^{-1} (above the CMC of P123), two peaks appear at 330.6 and 344.8 nm in the curve 2, due to the presence of P123 micelles in solution. For the spectrum of venlafaxine in the curve 3, a single and sharp emission peak is centered at 300 nm which is the characteristic peak of venlafaxine. The fluorescence intensity (value of ordinate) can reflect the concentration of venlafaxine by using the calibration curve. The curve 4 shows the emission spectrum of a mixed solution of venlafaxine and P123. Three peaks appear at the special wavelengths which could be distinctly identified as the combination of venlafaxine and P123. However, there are still very small shape changes, such as the intensity of the peak at 344.8 nm decreases and becomes lower than that of the peak at 330.6 nm, suggesting the microstructural change of P123 micelles due to the strong interaction with venlafaxine. Referring to the curve 5, the spectra of one typical experimental release curve, there is only one characteristic peak of venlafaxine at 300 nm, which suggests that the existence of P123 in MCFs would not cause interference. Combining with the thermogravimetric analysis result (as shown in Fig. S2), it suggests very little P123 would diffuse from the pores of MCF carriers along with the venlafaxine during the venlafaxine releasing process.

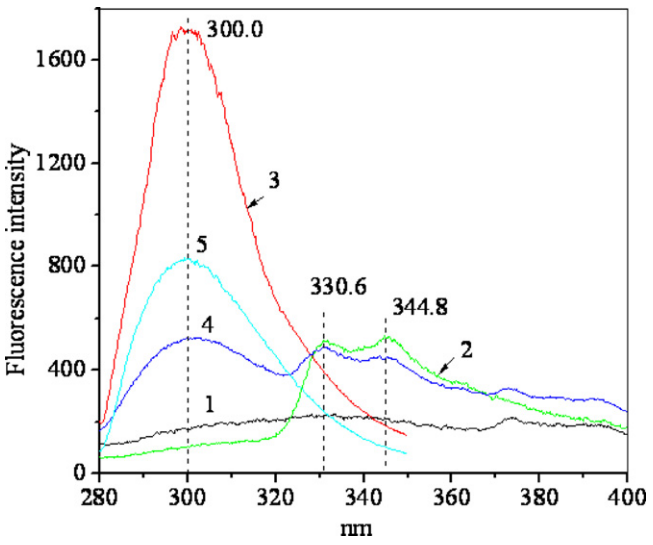

Fig. 6. Fluorescence emission spectra of P123, venlafaxine and their mixture at 37 °C. λ_{ex} = 237 nm. (1) 1 mg L^{-1} P123, (2) 10 mg L^{-1} P123, (3) 4 μg mL^{-1} venlafaxine, (4) a mixed aqueous solution of venlafaxine and P123, (5) one typical experimental release curve.

3.2.2. Controlled-release performance of venlafaxine from the MCFs with P123 template

A Food and Drug Administration (FDA) Guidance for Industry (US Department of Health and Human Services, 2000) concerning in vivo bioavailability and bioequivalence studies for immediate-release solid oral dosage forms suggested that the stability of drugs in gastrointestinal tract may be confirmed by incubating the drug substance in gastric and intestinal fluids at 37 °C for a period, e.g., 1 h in SGF and 3 h in SIF. Faustino et al. (Asafu-Adjaye et al., 2007) studied the stability of venlafaxine in the gastrointestinal tract. Their study suggested that venlafaxine would be stable in gastrointestinal tract and venlafaxine loss might take place by membrane permeation rather than a gastrointestinal degradation process. Hence, the release studies were performed in SGF at 37 °C for 1 h and in SIF at 37 °C for 12 h, respectively.

Fig. 7 shows the release profiles of venlafaxine from VEN-DH-MCF-P123-12, VEN-DH-MCF-P123-2 and VEN-DH-P123-0.5 in SGF and SIF systems. Focusing on the insert of 1 h release performance, in the acidic SGF medium, the initial release percents of venlafaxine from three drug carriers are significantly different, namely, ca. 8% for VEN-DH-MCF-P123-0.5, ca. 15% for VEN-DH-MCF-P123-2 and ca. 22% for VEN-DH-MCF-P123-12, which reflects the phenomenon that the more amounts of P123 remained, the lower initial release percents of venlafaxine. This trend continued to the end of 1 h release in SGF. It suggests that increasing the amount of P123 in carriers could influence the controlled-release of venlafaxine in SGF. In contrast, in neutral SIF medium, for VEN-DH-P123-2 and VEN-DH-P123-0.5, their initial release percents are almost the same, ca. 17% and 18%. However, for VEN-DH-MCF-P123-12, it significantly increases to ca. 37%, which suggests that the increasing amount of P123 also could delay the release of venlafaxine in SIF. Moreover, it shows that the values of release percent from the three carriers in SIF are all higher than that in SGF medium at the same time. This is illustrated by the case of VEN-DH-MCF-P123-2 which had the highest loading capacity of three carriers, about 36% of venlafaxine is released after 1 h of incubation in SGF, whereas about 45% departs from the carrier in SIF in the same time. Finally, ca. 52%

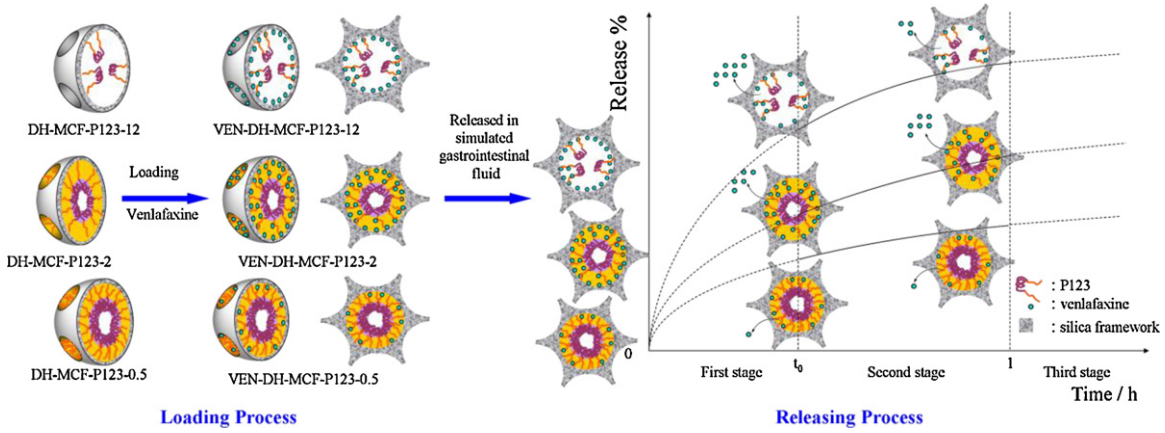

Scheme 2. Schematic representation of the mechanism for the loading and the releasing processes of MCFs with different amount of P123 template remained.

of venlafaxine is released after 12 h of incubation in SIF from the three carriers, which implies the good release efficiency. The above performances of the venlafaxine delivery systems with P123 template partially preserved were quite attractive, because it showed synergistic effects on both the loading capacity and the controlled-release. Meanwhile, by keeping suitable amount of P123 remaining in MCFs, it saved the consumption of raw materials, energies and fabrication time; and also increased the yield and characteristics of products, which will be particularly important for the future applications.

3.2.3. *Mechanism of the synergistic effect of P123 template on loading and controlled-release of venlafaxine*

To understand the synergistic effect of P123 template on the controlled-release, the mechanisms of both the loading and the releasing behaviors of venlafaxine were tentatively investigated. As a typical amphiphilic triblock copolymer with hydrophilic PEO blocks and hydrophobic PPO block, P123 can easily form micelles in aqueous solution. Hioka et al. (2002) reported P123 can enhance the solubility of a benzoporphyrin derivative inside its micelle core. After the loading process, venlafaxine would be stuck on the P123 chains due to the hydrogen bond between the two molecules, while the remainder would be absorbed at the framework surface of the silica MCF due to the interaction between the positive charge of ammonium groups of venlafaxine (as shown in Fig. 1) and the negative charge of the surface silanol groups.

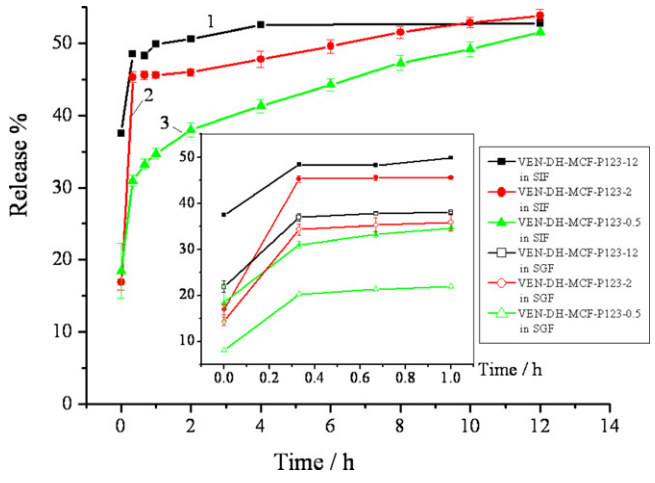

Fig. 7. Comparison of venlafaxine release behaviors from the drug carriers in SIF. (1) VEN-DH-MCF-P123-12, (2) VEN-DH-MCF-P123-2, (3) VEN-DH-MCF-P123-0.5. The insert is the enlargement of venlafaxine release behaviors from the drug carriers in both SIF and SGF within the initial 1 h.

As shown in Scheme 2, with increasing extraction time, the amount of P123 remaining in DH-MCF-P123-0.5, DH-MCF-P123-2 and DH-MCF-P123-12 decreases gradually, while the free volume in the pore increases. So the presence of P123 has two competitive effects on the drug loading. The positive one is to provide more active points that could capture the drug molecules in pores to increase the loading capacity; while the negative one is the steric effect that inhibits the loading process. As a result, DH-MCF-P123-2 has the maximum loading capacity among these three samples. While for DH-MCF-P123-12, with relative low P123 amount in mesopores, most venlafaxine can only be absorbed at the framework surface of the silica MCF through the interaction between venlafaxine and hydroxysilane; but for DH-MCF-P123-0.5, the mesopores are filled with P123 micelles and the steric effect obstructs the entrance of venlafaxine into the pores leading to the sharp decrease of loading capacity. Therefore the choice of carrier with appropriate amount of P123 is quite important in optimizing the drug loading.

After the loading process, the three carriers display different release performances. From the first data of the release profiles, corresponding to the time of t_0, for VEN-DH-MCF-P123-12, the initial burst is unavoidable because the interconnected pore structure of MCFs facilitates the drug fast diffusion. For VEN-DH-MCF-P123-2, suitable amounts of P123 remaining effectively hinder the drug release, which occurs through the steric effect for venlafaxine adsorbed on the silica framework surface, and also through the interaction for venlafaxine stuck on P123 chains. Thus the release percentage is much lower than that of VEN-DH-MCF-P123-12. For VEN-DH-MCF-P123-0.5, larger amounts of P123 present in pores obstruct the release process to a greater extent and lead to the lowest release percent at the first stage. At the second stage, namely, the time interval between t_0 and 1 h, for VEN-DH-MCF-P123-12, the release rate becomes slow since the concentration gradient of venlafaxine has been reduced after the initial burst. For VEN-DH-MCF-P123-2 and VEN-DH-MCF-0.5, venlafaxine is in a sustained release because of the steric effect from P123 and the interaction between the venlafaxine and P123. At the third stage, after the first 1 h, venlafaxine is released from the three carriers with relative slower rate till the end.

Moreover, comparing the release rate of venlafaxine in SGF and in SIF, the later was much faster than the former. In the acid SGF solution, because of the electrostatic repulsion between the positive hydrogen cations and the positive ammonium group of the venlafaxine, venlafaxine would be inhibited to release. Meanwhile, as Lettow et al. (2000) proposed, the presence of HCl would

dehydrate the PEO segments and result in a morphology contraction of P123 micelles. So the contraction of P123 chains in the acid SGF would produce stronger interaction with venlafaxine due to the closer contact sites, consequently, the release rate is reduced. As a contrast, in neutral SIF medium, PEO segments were relaxing and the interaction with the venlafaxine was lower than that in the SGF, which resulted in the faster release rate. So the presence of P123 chains in mesopores with different geometry would affect the drug loading capacity as well as the corresponding release behaviors.

4. Conclusions

In this paper, we demonstrated an easily achieved controlled-release system by partially extracting the P123 template from MCF materials. Appropriate amounts of P123 chains remained in MCF showed an efficient synergistic effect on both the loading and the controlled-release of venlafaxine. In the case of VEN-DH-MCF-P123-2, the loading capacity of venlafaxine can be the maximum of 90.87%. Meanwhile, in SGF medium, only ca. 15% of venlafaxine was released at the beginning and 36% was released after 1 h. In SIF medium, initially, ca. 18% of venlafaxine was released and 52% was released after 12 h. In contrast, for VEN-DH-MCF-P123-12 with the lowest P123 amount, the loading capacity decreased to 80.34%, while ca. 22% of venlafaxine was released at the beginning and 38% was released after 1 h in SGF, whereas for VEN-DH-MCF-P123-0.5 with the largest P123 amount, the drug loading capacity significantly decreased to 24.53%. P123 template remained in MCF showed two contributions in providing more active points to capture venlafaxine through interaction in the drug loading; as well as in obstructing the burst release of venlafaxine through the steric hindrance in the controlled-release, respectively. Since the silica-based drug release system and P123 are harmless for humans, and the convenient synthesis route and low energy consumption, we expect MCFs with appropriate amounts of P123 template remaining would be a promising controlled-release delivery for pharmaceuticals.

Acknowledgements

Financial support for this work was provided by the National Natural Science Foundation of China (Nos. 21076071 and 21176066) and the 111 Project (Grant No. B08021) of China. We also appreciated the suggestions of Prof. Richard Schwenz from the University of Northern Colorado.

Appendix A. Supplementary data

Supplementary data associated with this article can be found, in the online version, at doi:10.1016/j.ijpharm.2011.12.048.

References

Antochshuk, V., Jaroniec, M., 1999. Simultaneous modification of mesopores and extraction of template molecules from MCM-41 with trialkylchlorosilanes. Chem. Commun., 2373–2374.

Asafu-Adjaye, E.B., Faustino, P.J., Tawakkul, M.A., Anderson, L.W., Yu, L.X., Kwon, H., Volpe, D.A., 2007. Validation and application of a stability-indicating HPLC method for the in vitro determination of gastric and intestinal stability of venlafaxine. J. Pharm. Biomed. Anal. 43, 1854–1859.

Cao, S., Zhu, Y., Wu, J., Wang, K., Tang, Q., 2010. Preparation and sustained-release property of triblock copolymer/calcium phosphate nanocomposite as nanocarrier for hydrophobic drug. Nanoscale Res. Lett. 5, 781–785.

Drug Topics, 2008. Top 200 brand drugs by units in 2007. Available from: http://drugtopics.modernmedicine.com/drugtopics/PharmacyFactsAndFigures/ArticleStandard/article/detail/491210.

EFFEXOR XR® (venlafaxine hydrochloride) Extended-Release Capsules' label. Wyeth Pharmaceuticals Inc. Available from: http://labeling.pfizer.com/showlabeling.aspx?id=100.

Gillies, E.R., Fréchet, J.M.J., 2005. Dendrimers and dendritic polymers in drug delivery. Drug Discov. Today 10, 35–43.

Gonzalez, O., Berry, J.T., McKnight-Eily, L.R., Strine, T., Edwards, V.J., Lu, H., Croft, J.B., 2010. Current depression among adults—United States, 2006 and 2008. MMWR Morb. Mortal. Wkly. Rep. 59, 1229–1235.

Gou, M., Men, K., Shi, H., Xiang, M., Zhang, J., Song, J., Long, J., Wan, Y., Luo, F., Zhao, X., Qian, Z., 2011. Curcumin-loaded biodegradable polymeric micelles for colon cancer therapy in vitro and in vivo. Nanoscale 3, 1558–1567.

Gregg, S.J., Sing, K.S.W., 1982. Adsorption, Surface Area and Porosity, 2nd ed. Academic press, London.

Gyenes, T., Torma, V., Gyarmati, B., Zrínyi, M., 2008. Synthesis and swelling properties of novel pH-sensitive poly(aspartic acid) gels. Acta Biomater. 4, 733–744.

Han, Y., Lee, S.S., Ying, J.Y., 2007. Spherical siliceous mesocellular foam particles for high-speed size exclusion chromatography. Chem. Mater. 19, 2292–2298.

Hioka, N., Chowdhary, R.K., Chansarkar, N., Delmarre, D., Sternberg, E., Dolphin, D., 2002. Studies of a benzoporphyrin derivative with Pluronics. Can. J. Chem. 80, 1321–1326.

Horcajada, P., Rámila, A., Pérez-Pariente, J., Vallet-Regí, M., 2004. Influence of pore size of MCM-41 matrices on drug delivery rate. Micropor. Mesopor. Mater. 68, 105–109.

Hrubý, M., Konák, C., Ulbrich, K., 2005. Polymeric micellar pH-sensitive drug delivery system for doxorubicin. J. Control. Release 103, 137–148.

Jain, T.K., Roy, I., De, T.K., Maitra, A., 1998. Nanometer silica particles encapsulating active compounds: a novel ceramic drug carrier. J. Am. Chem. Soc. 120, 11092–11095.

Kabanov, A.V., Batrakova, E.V., Alakhov, V.Y., 2002. Pluronic® block copolymers as novel polymer therapeutics for drug and gene delivery. J. Control. Release 82, 189–212.

Kataoka, K., Harada, A., Nagasaki, Y., 2001. Block copolymer micelles for drug delivery: design, characterization and biological significance. Adv. Drug Deliv. Rev. 47, 113–131.

Keltjens, R., Picha, F., Escoi, J.C., 2003. Venlafaxine base, United States Patent Application 20030191347.

Kim, S., Kwon, K., Kwon, I.C., Park, K., 2009. Nanotechnology in drug delivery: past, present, and future. In: Villiers, M.M., Aramwit, P., Kwon, G.S. (Eds.), Nanotechnology in Drug Delivery. Springer, New York, pp. 581–596.

Lasic, D.D., Vallner, J.J., Working, P.K., 1999. Sterically stabilized liposomes in cancer therapy and gene delivery. Curr. Opin. Mol. Ther. 1, 177–185.

Lee, E.S., Shin, H.J., Na, K., Bae, Y.H., 2003. Poly(-histidine)-PEG block copolymer micelles and pH-induced destabilization. J. Control. Release 90, 363–374.

Lee, E.S., Na, K., Bae, Y.H., 2005. Doxorubicin loaded pH-sensitive polymeric micelles for reversal of resistant MCF-7 tumor. J. Control. Release 103, 405–418.

Lettow, J.S., Han, Y.J., Schmidt-Winkel, P., Yang, P., Zhao, D., Stucky, G.D., Ying, J.Y., 2000. Hexagonal to mesocellular foam phase transition in polymer-templated mesoporous silicas. Langmuir 16, 8291–8295.

Liu, M., Fréchet, J.M.J., 1999. Designing dendrimers for drug delivery. Pharm. Sci. Technol. Today 2, 393–401.

Liu, T.Y., Hu, S.H., Liu, K.H., Liu, D.M., Chen, S.Y., 2008. Study on controlled drug permeation of magnetic-sensitive ferrogels: effect of Fe_3O_4 and PVA. J. Control. Release 126, 228–236.

Lukens, W.W., Schmidt-Winkel, P., Zhao, D., Feng, J., Stucky, G.D., 1999. Evaluating pore sizes in mesoporous materials: a simplified standard adsorption method and a simplified Broekhoffâ-de Boer Method. Langmuir 15, 5403–5409.

Mal, N.K., Fujiwara, M., Tanaka, Y., 2003. Photocontrolled reversible release of guest molecules from coumarin-modified mesoporous silica. Nature 421, 350–353.

Matsumura, Y., Hamaguchi, T., Ura, T., Muro, K., Yamada, Y., Shimada, Y., Shirao, K., Okusaka, T., Ueno, H., Ikeda, M., Watanabe, N., 2004. Phase I clinical trial and pharmacokinetic evaluation of NK911, a micelle-encapsulated doxorubicin. Br. J. Cancer 91, 1775–1781.

Murdan, S., 2003. Electro-responsive drug delivery from hydrogels. J. Control. Release 92, 1–17.

Nakanishi, T., Fukushima, S., Okamoto, K., Suzuki, M., Matsumura, Y., Yokoyama, M., Okano, T., Sakurai, Y., Kataoka, K., 2001. Development of the polymer micelle carrier system for doxorubicin. J. Control. Release 74, 295–302.

Nasongkla, N., Bey, E., Ren, J., Ai, H., Khemtong, C., Guthi, J.S., Chin, S.F., Sherry, A.D., Boothman, D.A., Gao, J., 2006. Multifunctional polymeric micelles as cancer-targeted, MRI-ultrasensitive drug delivery systems. Nano Lett. 6, 2427–2430.

Panyam, J., Labhasetwar, V., 2003. Biodegradable nanoparticles for drug and gene delivery to cells and tissue. Adv. Drug Deliv. Rev. 55, 329–347.

Panyam, J., Zhou, W., Prabha, S., Sahoo, S.K, Labhasetwar, V., 2002. Rapid endo-lysosomal escape of poly(DL-lactide-co-glycolide) nanoparticles: implications for drug and gene delivery. FASEB J. 16, 1217–1226.

Park, J., 2002. Liposome-based drug delivery in breast cancer treatment. Breast Cancer Res. 4, 95–99.

Pasqua, L., Testa, F., Aiello, R., Cundari, S., Nagy, J.B., 2007. Preparation of bifunctional hybrid mesoporous silica potentially useful for drug targeting. Micropor. Mesopor. Mater. 103, 166–173.

Rosler, A., Vandermeulen, G.W., Klok, H.A., 2001. Advanced drug delivery devices via self-assembly of amphiphilic block copolymers. Adv. Drug Deliv. Rev. 53, 95–108.

Roy, I., Ohulchanskyy, T.Y., Pudavar, H.E., Bergey, E.J., Oseroff, A.R., Morgan, J., Dougherty, T.J., Prasad, P.N., 2003. Ceramic-based nanoparticles entrapping water-insoluble photosensitizing anticancer drugs: a novel drug-carrier system for photodynamic therapy. J. Am. Chem. Soc. 125, 7860–7865.

Sahoo, S.K., Labhasetwar, V., 2003. Nanotech approaches to drug delivery and imaging. Drug Discov. Today 8, 1112–1120.

Schmidt-Winkel, P., Lukens, W.W., Zhao, D., Yang, P., Chmelka, B.F., Stucky, G.D., 1999. Mesocellular siliceous foams with uniformly sized cells and windows. J. Am. Chem. Soc. 121, 254–255.

Schmidt-Winkel, P., Lukens, W.W., Yang, P., Margolese, D.I., Lettow, J.S., Ying, J.Y., Stucky, G.D., 2000. Microemulsion templating of siliceous mesostructured cellular foams with well-defined ultralarge mesopores. Chem. Mater. 12, 686–696.

Shahnawaz, S., Siddiqui, Z., Hoda, Q., 2010. Sensitive spectrofluorimetric method of analysis for venlafaxine in spiked rat plasma and formulations. J. Fluoresc. 20, 821–825.

Slowing, I.I., Vivero-Escoto, J.L., Wu, C.W., Lin, V.S., 2008. Mesoporous silica nanoparticles as controlled release drug delivery and gene transfection carriers. Adv. Drug Deliv. Rev. 60, 1278–1288.

Sonoda, A., Nitta, N., Ohta, S., Nitta-Seko, A., Morikawa, S., Tabata, Y., Takahashi, M., Murata, K., 2010. Controlled release and antitumor effect of Pluronic F127 mixed with cisplatin in a rabbit model. Cardiovasc. Inter. Radiol. 33, 135–142.

Tang, J., Slowing, I.I., Huang, Y., Trewyn, B.G., Hu, J., Liu, H., Lin, V.S.Y., 2011. Poly(lactic acid)-coated mesoporous silica nanosphere for controlled release of venlafaxine. J. Colloid Interface Sci. 360, 488–496.

Torchilin, V.P., Lukyanov, A.N., Gao, Z., Papahadjopoulos-Sternberg, B., 2003. Immunomicelles: targeted pharmaceutical carriers for poorly soluble drugs. Proc. Natl. Acad. Sci. U.S.A. 100, 6039–6044.

US Department of Health and Human Services, Food and Drug Administration, Center for Drug Evaluation and Research, 2000. Guidance for Industry, Waiver of In Vivo Bioavailability and Bioequivalence Studies for Immediate-release Solid Oral Dosage Forms Based on a Biopharmaceutics Classification System. Available from: http://www.fda.gov/downloads/Drugs/GuidanceComplianceRegulatoryInformation/Guidances/ucm070246.pdf.

USP-NF, 2005. Test solutions. Unites States Pharmacopoeia 28/National Formulary 23. Available from: http://www.usp.org.

Vallet-Regí, M., Rámila, A., del Real, R.P., Pérez-Pariente, J., 2000. A new property of MCM-41: drug delivery system. Chem. Mater. 13, 308–311.

Vivero-Escoto, J.L., Slowing, I.I., Trewyn, B.G., Lin, V.S.Y., 2010. Mesoporous silica nanoparticles for intracellular controlled drug delivery. Small 6, 1952–1967.

Wanka, G., Hoffmann, H., Ulbricht, W., 1994. Phase diagrams and aggregation behavior of poly(oxyethylene)-poly(oxypropylene)-poly(oxyethylene) triblock copolymers in aqueous solutions. Macromolecules 27, 4145–4159.

Wellington, K., Perry, C.M., 2001. Venlafaxine extended-release: a review of its use in the management of major depression. CNS Drugs 15, 643–669.

Xu, W., Gao, Q., Xu, Y., Wu, D., Sun, Y., Shen, W., Deng, F., 2008. Controlled drug release from bifunctionalized mesoporous silica. J. Solid State Chem. 181, 2837–2844.

Yang, Y.J., Tao, X., Hou, Q., Ma, Y., Chen, X.L., Chen, J.F., 2010. Mesoporous silica nanotubes coated with multilayered polyelectrolytes for pH-controlled drug release. Acta Biomater. 6, 3092–3100.

Yokoyama, M., Fukushima, S., Uehara, R., Okamoto, K., Kataoka, K., Sakurai, Y., Okano, T., 1998. Characterization of physical entrapment and chemical conjugation of adriamycin in polymeric micelles and their design for in vivo delivery to a solid tumor. J. Control. Release 50, 79–92.

Zhang, J., Bhat, R., Jandt, K.D., 2009. Temperature-sensitive PVA/PNIPAAm semi-IPN hydrogels with enhanced responsive properties. Acta Biomater. 5, 488–497.

Zhang, Y., Jiang, T., Zhang, Q., Wang, S., 2010. Inclusion of telmisartan in mesocellular foam nanoparticles: drug loading and release property. Eur. J. Pharm. Biopharm. 76, 17–23.

Zhang, Y., Zhang, J., Jiang, T., Wang, S., 2011. Inclusion of the poorly water-soluble drug simvastatin in mesocellular foam nanoparticles: drug loading and release properties. Int. J. Pharm. 410, 118–124.

Zhu, Y., Shi, J., Shen, W., Dong, X., Feng, J., Ruan, M., Li, Y., 2005. Stimuli-responsive controlled drug release from a hollow mesoporous silica sphere/polyelectrolyte multilayer core–shell structure. Angew. Chem. 117, 5213–5217.